Adaptive Transient and CW RF Interference Mitigation in HF OTH Radar: Experimental Results

Pavel Turcaj, Yuri I. Abramovich and Gordon J. Frazer

Abstract—We introduce an adaptive technique for the joint mitigation of transients and continuous-wave radio-frequency co-channel interference (CW RFI) in high-frequency (HF) over-the-horizon radars (OTHRs). The performance of this technique is illustrated using data from an operational surface-wave radar (SECAR) and from recent experimental trials with sky-wave (SW) and sky-wave–line-of-sight (SKYLOS) HF OTHRs.

I. PROBLEM FORMULATION

It is the various propagation modes of HF signals (5–30 MHz), involving sky-wave (ionospheric), surface-wave (over the highly conductive ocean surface) and line-of-sight propagation, that necessitate the variety of OTHR configurations and architectures. In addition to conventional sky-wave radars (such as the Australian JORN system [1]) and surface-wave radars (such as the Australian SECAR radar [2]), radar systems that exploit sky-wave–line-of-sight (SKYLOS) and sky-wave–surface-wave (SKYSURF) modes are under investigation. Each of these systems addresses different operational requirements and therefore their architectures may vary significantly. For instance, receive antenna arrays in modern sky-wave radars may consist of several hundreds of digitised sensors; in surface-wave radars the number rarely exceeds a few dozen, whilst a SKYLOS configuration may involve just a single receive element.

Yet each of these radar systems has to operate within the environment congested by human and natural interferences. The main sources of natural interferences are lightning strikes (atmospherics) which could be of very high power, with a duration of only a few (often just one) repetition intervals. Due to high sensitivities and receive antenna gains, modern sky-wave radars often encounter a number of such impulsive-noise strikes in their main beams. Surface-wave radars usually operate in littoral areas, such as the Northern Australia coast that is infamous for its high intensity thunderstorm activity during the "wet season" [3]. Passive reflections from transient phenomena, such as meteors, act similarly to lightning strikes, but usually corrupt a limited number of range cells over a limited number of repetition periods.

Therefore, transients (lightning strikes and meteor reflections) corrupt a small number of repetition intervals over a small set (meteor reflections) or the entire set of range cells. Human interference can be either transient-like or CW RFI.

While significantly different in their time-frequency properties, the source of the all the above interferences are well-localised in space (*ie*. arrive from particular directions). The space-time/frequency distinctions between transients, CW RFI and "intrinsic" radar returns (targets and clutter) are used in interference mitigation strategies. In particular, transients that arrive via a sidelobe of the antenna main beam may be removed both by spatial filtering (steering a null in its direction), or by temporal processing that excludes the corrupted processing repetition intervals (PRIs, sweeps) from coherent processing. Obviously, transients that arrive via the main beam could be dealt with only by temporal processing, since placing a null in the main-beam antenna direction for an entire coherent processing interval (CPI) will destroy radar performance. Therefore, in the multi-element antenna arrays of modern sky-wave radars, one has to treat transients arriving via the main beam by temporal adaptive techniques, leaving the remainder for spatial adaptive processing together with CW RFI removal. Indeed, the number of very strong transients affecting a given main beam via sidelobes is limited and the number of spatial degrees of freedom (antenna elements) in such radars significantly exceeds the number of waveform repetition intervals. Therefore, mitigation of "sidelobe transients" in these radars is much more efficient by spatial, rather than by temporal processing [3].

In SKYLOS configurations with their very limited number of antenna sensors, the rationale behind the need to treat transients and CW RFI separately is different. In this configuration, the number of antenna elements specifies the number of dominant CW RFI sources that could be removed only by spatial adaptive processing. Obviously, transients must be dealt with by temporal adaptive processing in order not to overload the very limited number of spatial degrees of freedom. Therefore, the interaction between spatial and temporal adaptive processing for joint transient and CW RFI mitigation is not straight-forward and must be properly designed. In this paper we report on such a design and provide experimental verification of its efficiency.

II. METHOD DESCRIPTION

The mitigation algorithm which combines adaptive transient and CW RFI mitigation, may be outlined as follows:

1. Detect sweeps and ranges affected by transients arriving via the main beam (separately for each finger-beam within the coverage).
2. Select training ranges and sweeps that are free of transients affecting that particular beam direction, to be used as beam-specific training data for CW RFI mitigation via adaptive beamforming, and remove clutter.
3. Using the beam-specific estimates of the spatial covariance matrix $R(\Theta_j)$, perform adaptive beamforming for CW RFI and "sidelobe-transient" mitigation.
4. Perform transient mitigation by adaptive temporal processing at the output of the adaptive beamformer with

mitigated CW RFI and "sidelobe transients".

For SKYLOS configurations, steps 1 and 2 must be performed for each antenna element (*ie*. no beamforming).

A. Impulsive Noise and Transient Detection

In some cases (surface-wave radars, for example) access to ranges not occupied by ground clutter may be available. These "training" ranges may be directly used for detecting lightning strikes (impulsive noise) and RFI training data. Yet, transients cannot be detected in the same way, since they are affecting only limited number of ranges (and usually operationally important ones). Moreover, in most current OTHR systems, digital range processing is performed for operationally important ranges only. Therefore, transient detection has to be performed within the background of strong clutter reflection.

To achieve this, an adaptive moving-target-indicator (MTI) filter is designed at the output of each conventionally formed finger-beam, with the minimal number of sweeps involved

$$W(j,d) = \frac{\hat{R}_n^{-1}(j,d)e_1}{e_1^T \hat{R}_n^{-1}(j,d)e_1} \qquad (1)$$

where

$$\hat{R}_n(j,d) = \sum_{l=1}^{N-n} [X_l^d(j)(X_l^d(j))^H + JX_l^d(j)(X_l^d(j))^H J] \quad (2)$$

with

$$X_l^d(j) = [x_l^d(j), x_{l+1}^d(j), \ldots, x_{l+n-1}^d(j)]^T \qquad (3)$$

and $x_l^d(j)$ is the complex number that corresponds to the l-th repetition period sample for the d-th range cell at the output of the j-th finger-beam.

The shortest "memory" n of the MTI filter is required since it specifies the number of sweeps affected by a single impulse at the output of the MTI filter. This number depends on the radar operation mode, but even for a ship detection mode with the longest sweeps, the sufficient number is shown to be reasonably small.

Simple power comparison of the strong transients clearly detectable at the output of a single antenna element and a given beam allows us to discriminate such a strike as a "main-beam" or a "sidelobe" one. Typically though, most of the transients detected are "main-beam" ones due to the high gain and low sidelobe level of conventional beamforming. Transients and impulsive-noise strikes are detected at the output of the MTI filter, and we declare that the entire sweep is affected by impulsive noise (not a transient) if most of the range cells are affected in the same sweep.

B. CW RFI Adaptive Mitigation

The main distinction of the proposed technique and conventional adaptive beamforming is the beam-dependent selection of the training data at the output of the antenna array elements. Specifically, when training data is collected for adaptive beamforming in the direction Θ_j, all transients (*ie*. affected range cells and repetition intervals) detected in Stage A are removed. Since for each finger-beam direction, the set of affected range cells and repetition intervals is different, we end up with a beam-tailored set of training data. If, say, a conventional LSMI beamformer is used, then the M-element adaptive beamformer vector is calculated as

$$\hat{W}(\Theta_j) = \frac{\left[\hat{R}_l(\Theta_j)\right]^{-1} S(\Theta_j)}{S^H(\Theta_j)\left[\hat{R}_l(\Theta_j)\right]^{-1} S(\Theta_j)} \qquad (4)$$

where

$$\hat{R}_l(\Theta_j) = \sum_{k\tau \in \Omega_j} X_{k,\tau}(\Theta_j)X_{k,\tau}^H(\Theta_j) + \alpha I_M \qquad (5)$$

α is loading factor; k,τ is the selected range and repetition interval; $X_{k,\tau}(\Theta_j) \in C^{M\times 1}$ is the M-variate vector collected at the output of the M-element antenna array at the range k and repetition interval τ at the output of the MTI filter; Ω_j is the set of all range cells and repetition intervals, selected as training for the direction Θ_j.

Note that a more sophisticated time-varying adaptive techniques ("stochastically constrained" for example [4]) may be also applied using the direction-dependent set of training data.

C. Impulsive Noise and Transient Mitigation

As a result of CW RFI mitigation at the output of a particular adaptive beamformer, the clutter-to-noise ratio has increased. If required, steps A and B may now be repeated with better clutter mitigation and therefore weaker transient detection. Ultimately, when no further transients are detected, the RFI-cleared sweep data for each range cell and beam output may be once again used for clutter covariance matrix estimation via "sliding window" forward-backward averaging over the entire CPI. In this averaging, similar to (2), sweeps affected by transients are replaced by zeroes, and sufficiently homogeneous neighbouring range cells data may be averaged over to improve the statistical reliability of this covariance matrix estimate R_d. In contrast with the MTI filter with minimal filter memory, the dimension of the covariance matrix k is selected close to the maximum, $k \sim N/3$, where N is the number of sweeps in the CPI. The rationale behind maximal order k selection is that within the k-long "sliding window" the number of "missing" sweeps affected by transients m is still significantly smaller than the number of "proper" clutter samples, *ie*.

$$k - m \gg m \qquad (6)$$

which means that interpolation of the "missing" clutter sweeps is efficient.

Let us introduce a $k \times (k-m)$ incidence matrix H_m that is constructed from the identity matrix with m deleted rows at positions that correspond to the "missing" sweeps. Then the adaptive prediction filter that generates an estimate of the p-th missing data is defined as

$$W_p^d = \left[H_m^T \hat{R}_d H_m\right]^{-1} H_m r_p^d; \qquad p = 1, \ldots, m. \quad (7)$$

where r_p^d is the p-th column of the M-variate matrix $\hat{R}_d$. Correspondingly, the estimate $\hat{x}_p^d$ (for the range cell d and the particular beam) is calculated as

$$\hat{x}_p^d = \hat{W}_p^{dH} H_m^T X^d; \qquad p = 1, \ldots, m. \qquad (8)$$

where X^d is the k-variate data within the "sliding window", and $H_m^T X^d$ is the vector of $(k - m)$ "proper" sweeps.

When the number of sweeps affected by transients is reasonable high $(K - m \gtrsim m)$, this step may be repeated, with predicted clutter values used instead of zeroes in the covariance matrix estimate.

We have described the main principles of our suggested routine, while it should be clear that the implemented operational routine requires some "fine tuning".

III. EXPERIMENTAL RESULTS

An adaptive algorithm similar to one described above has been successfully implemented as an operational real-time algorithm in the SECAR surface-wave radar. The joint transient and CW RFI mitigation algorithm described above was implemented as a prototype algorithm for sky-wave radar in ship mode and also as a post-processing algorithm in the SKYLOS experiment. In Fig 1, we illustrate the results of conventional beamforming and Doppler processing for surface-wave radar, compared with the post-adaptive processing results. A significant improvement in subclutter visibility is clearly seen.

Fig 1(d) shows "non-Dopplerised" data (range-time data) in which one can clearly observe impulses created by lightning strikes in the "negative ranges" (below the direct-wave signal). As mentioned, in this application Step A is used for detecting transients created by reflections from meteors.

In Fig 2, we present the results of sky-wave radar data processing, collected in ship mode. We compare results of conventional beamforming and Doppler processing (Fig 2(a)), with the results of transient-mitigation only (Fig 2(b)) and the results of joint transient and CW RFI mitigation (Fig 2(c)). We again observe a significant reduction in the "noise floor" power. In particular, a transponder signal became clearly detectable as a result of the adaptive processing.

Finally, we present results using data from recent SKYLOS trials that occurred during the launch of NASA Space Shuttle mission STS-118. The space shuttle was launched on 8 August 2007 at 22:36:46 UTC. We have processed the collected data by the above described method using one element (channel data), two and three elements (adaptively beamformed data). For the beamformed data we used only beam pointing in the direction of the space shuttle. We used dwells consisting of 256 sweeps, with the shift between dwells being 32 sweeps (ie. two consecutive dwells share 224 sweeps). We processed ten minutes of data which gives just over 920 dwells to evaluate.

In Fig 4(a), we show channel 1 after conventional processing. On the y axis we show time; each line represents one dwell. On the x axis we show Doppler cuts for six ranges (17–22) (ie. the first 256 pixels are all the Dopplers for range 17, second 256 pixels are all the Dopplers for range 18 etc). Fig 4(b) shows channel 1 after impulsive-noise and transient mitigation only (as we need more than one element for SAP); Fig 4(c) shows adaptively beamformed data using channel 1 and 2; Fig 4(d) shows adaptively beamformed data using all three channels. The space shuttle track can be clearly seen in all three figures after our processing, whilst some portions of the track are not visible after conventional processing.

Fig 3 compares the median noise levels of the conventionally processed first channel, impulsive-noise mitigation of the first channel, impulsive and spread-noise mitigation using the first and second channels, and impulsive and spread noise mitigation using all three channels.

IV. CONCLUSIONS

The presented results demonstrate that the proposed combined adaptive processing technique gives a significant improvement of signal-to-noise ratio with respect to both transient and CW RFI in OTHRs with various configurations, specifically sky-wave, surface-wave and SKYLOS.

REFERENCES

[1] A. Cameron, "The jindalee operational radar network : Its architecture and surveillance capability," *IEEE Internnational Radar Conference*, pp. 692–697, 1995.

[2] S. Anderson, P. Edwards, P. Marrone, and Y. Abramovich, "Investigations with SECAR — a bistatic HF surface wave radar," in *Proc. IEEE RADAR-2003*, Adelaide, Australia, 2003, pp. 717–722.

[3] Y. Abramovich and P. Turcaj, "Impulsive noise mitigation in spatial and temporal domains for surface-wave over-the-horizon radar," in *Proc. ASAP-2001*, MIT Lincoln Laboratory, MA, USA, 2001, pp. 19–24.

[4] Y. Abramovich, N. Spencer, and A. Gorokhov, "Positive-definite Toeplitz completion in DOA estimation for nonuniform linear antenna arrays — Part II: Partially augmentable arrays," *IEEE Trans. Sig. Proc.*, vol. 47, no. 6, pp. 1502–1521, June 1999.

Yuri I. Abramovich (M'96–SM'06) received the Dipl.Eng. (Hons.) degree in radio electronics in 1967 and the Cand.Sci. degree (Ph.D. equivalent) in theoretical radio techniques in 1971, both from the Odessa Polytechnic University, Odessa (Ukraine), U.S.S.R., and in 1981, he received the D.Sc. degree in radar and navigation from the Leningrad Institute for Avionics, Leningrad (Russia), U.S.S.R.
From 1968 to 1994, he was with the Odessa State Polytechnic University, Odessa, Ukraine, as a Research Fellow, Professor, and ultimately as Vice-Chancellor of Science and Research. From 1994 to 2006, he was at the Cooperative Research Centre for Sensor Signal and Information Processing (CSSIP), Adelaide, Australia. Since 2000, he has been with the Australian Defence Science and Technology Organisation (DSTO), Adelaide, as Principal Research Scientist, seconded to CSSIP until its closure. His research interests are in signal processing (particularly spatio-temporal adaptive processing, beamforming, signal detection and estimation), its application to radar (particularly over-the-horizon radar), electronic warfare, and communication. He served as Associate Editor of *IEEE Transactions on Signal Processing* from 2002 to 2005.

Pavel Turcaj received the RNDr degree in numerical mathematics in 1989 from Charles University, Prague, Czechoslovakia and Ph.D degree in 1997 from the Flinders University, Adelaide, Australia.
From 1998 till 2006 he has been at the Cooperative Research Centre for Sensor Signal and Information Processing (CSSIP), Adelaide, Australia. Since 2006, he has been with the Adelaide Research and Innovation as Senior Researcher. His research interests are in signal processing for over-the-horizon radar (both surface-wave and sky-wave).

Gordon J. Frazer received the B.E. (elect.) (Hons.) degree from the University of Canterbury, New Zealand in 1982, the M.Eng.Sc degree from the University of Queensland, Brisbane in 1990 and the Ph.D. degree from Queensland University of Technology, Brisbane in 1996.
From 1982 to 1988 he was a communications engineer with the Queensland Electricity Commission working on communications and control problems in electricity transmission. This included design and implementation of custom modems using digital signal processors. From 1988 until 1990 he developed a variety of custom digital signal processor applications at Mosaic Electronics Pty. Ltd. Since 1990 he has been with the Intelligence, Surveillance and Reconnaissance Division, Part of the Australian Defence Science and Technology Organisation. He is presently a Principal Research Scientist and Research Leader of HF Radar Branch. His research interests are in radar design, signal analysis and array signal processing.
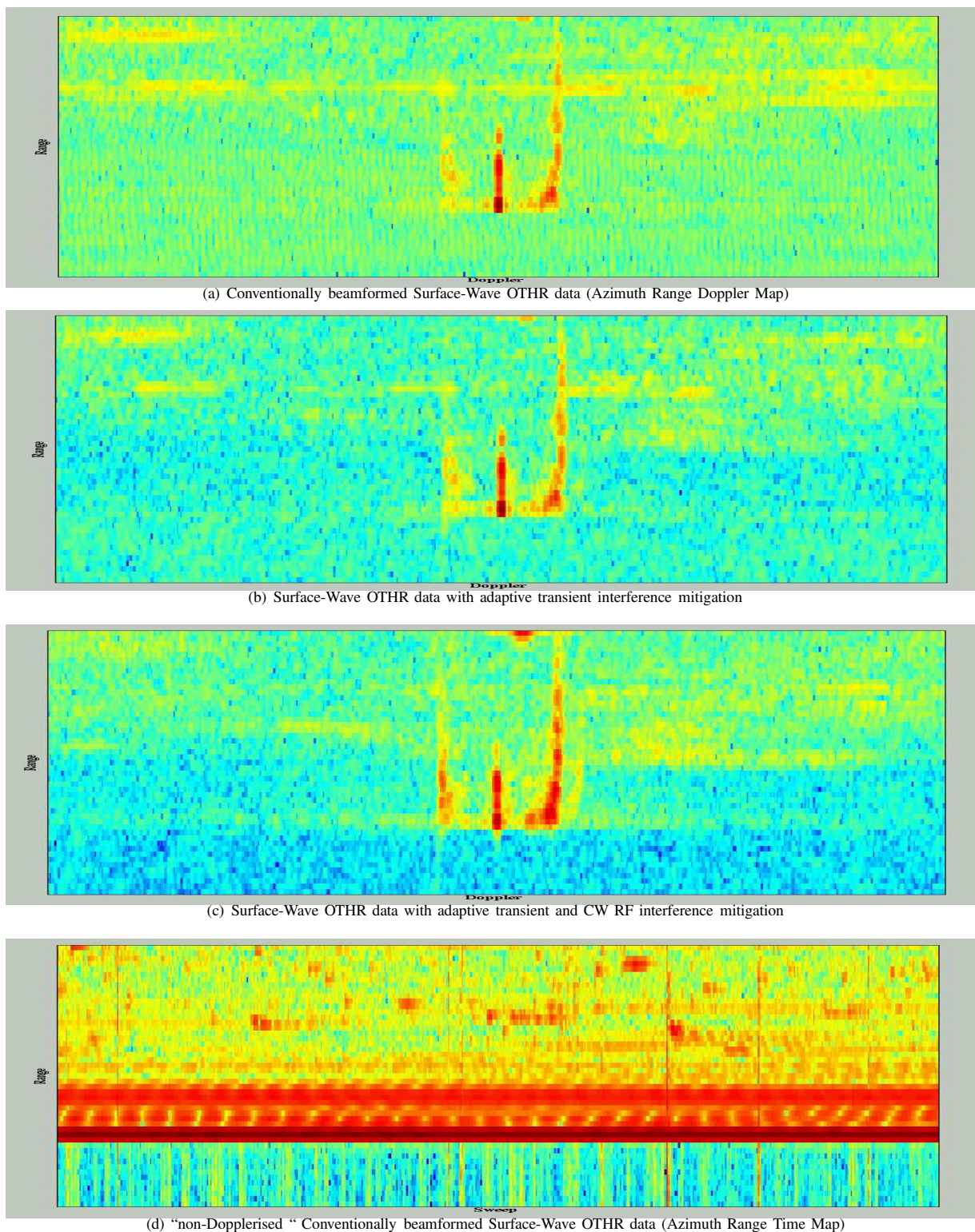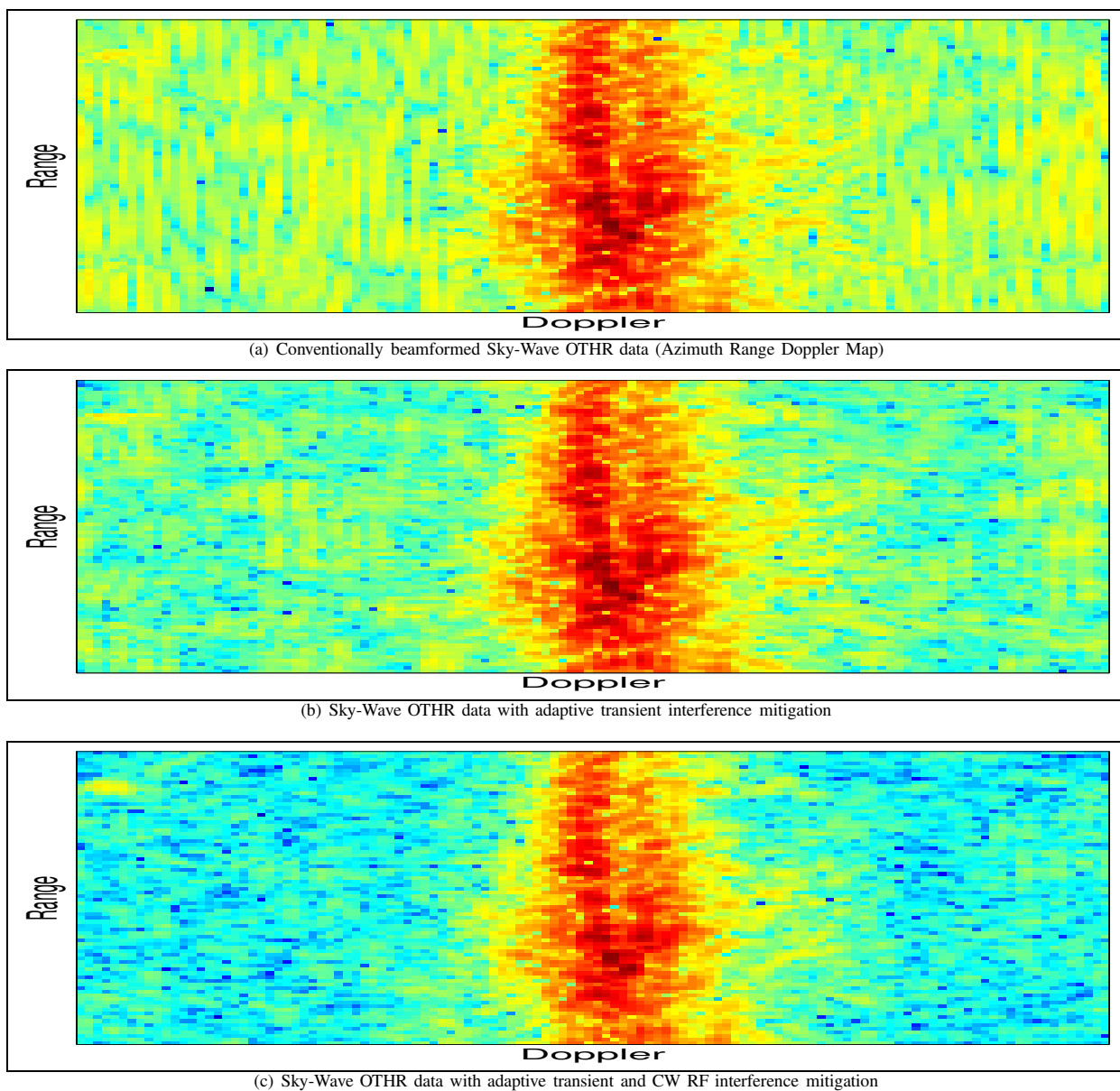
(a) Conventionally beamformed Surface-Wave OTHR data (Azimuth Range Doppler Map)

(b) Surface-Wave OTHR data with adaptive transient interference mitigation

(c) Surface-Wave OTHR data with adaptive transient and CW RF interference mitigation

(d) "non-Dopplerised " Conventionally beamformed Surface-Wave OTHR data (Azimuth Range Time Map)

Fig. 1.   Surface-Wave OTHR data.

(a) Conventionally beamformed Sky-Wave OTHR data (Azimuth Range Doppler Map)

(b) Sky-Wave OTHR data with adaptive transient interference mitigation

(c) Sky-Wave OTHR data with adaptive transient and CW RF interference mitigation

Fig. 2. Sky-Wave OTHR data.

Fig. 3. Comparison of median noise levels for SKYLOS data.

(a) Channel 1 conventional beamforming.

(b) Channel 1 after impulsive noise and transient mitigation.

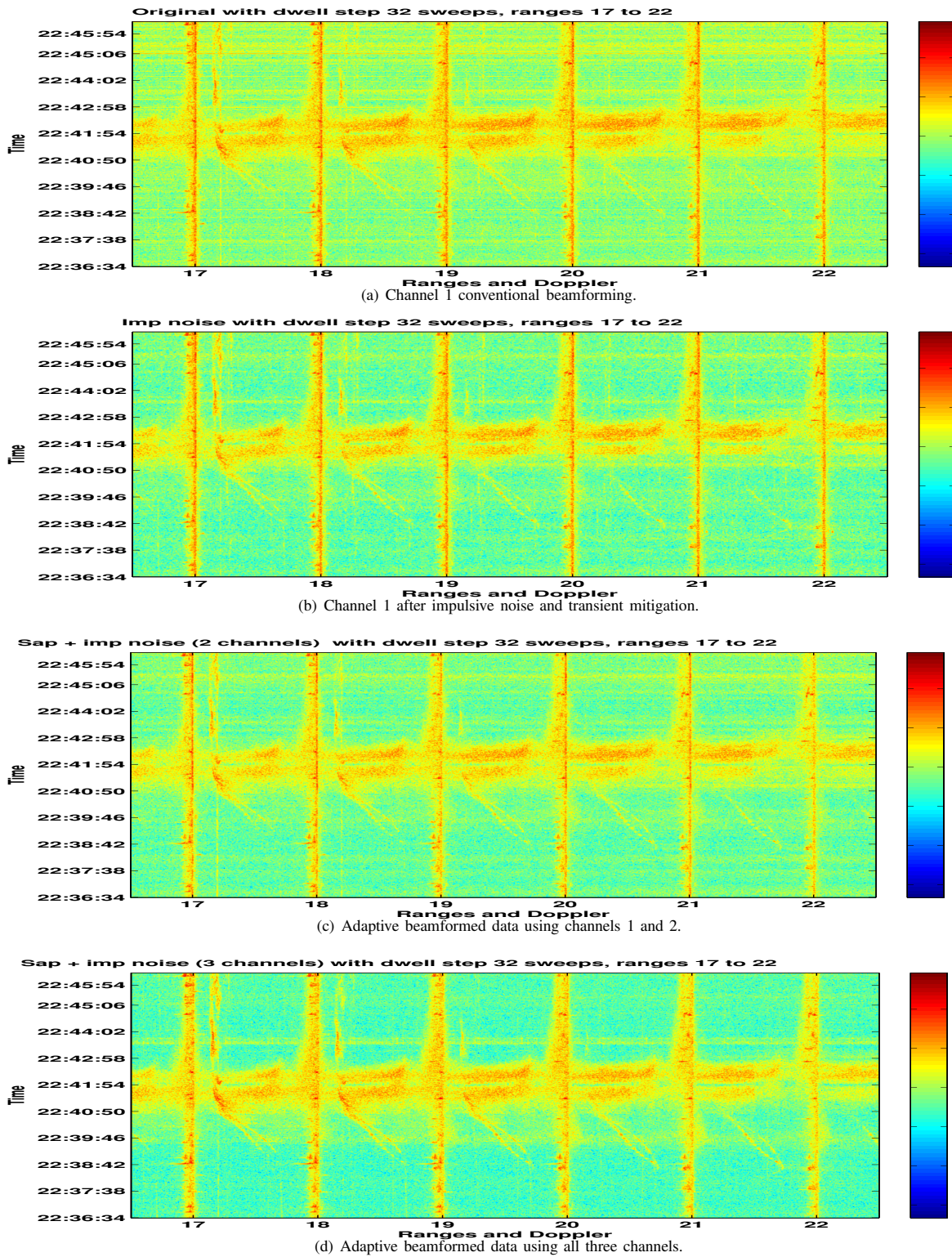(c) Adaptive beamformed data using channels 1 and 2.

(d) Adaptive beamformed data using all three channels.

Fig. 4.   Skylos OTHR data.